JOURNAL OF MATERIALS SCIENCE 21 (1986) 3071–3077

Martensite–austenite transformation in maraging steel alloys during tensile deformation and thermal cycling

M. A. KENAWY*, M. R. NAGY‡, E. M. SAKR*
*University College of Girls and ‡Faculty of Education, Ain Shams University, Cairo, Egypt

The effect of simultaneous additions of tungsten on the martensite (M) $\rightleftharpoons$ austenite (γ) transformation, taking place during tensile deformation under different constant stresses and thermal cyclic rates for Fe–Ni–Co based maraging steel alloys was studied. The strain rate sensitivity parameter m was found to be 1.0 and 0.6 for the M $\rightarrow$ γ and γ $\rightarrow$ M transformations, respectively. The interpretation of deformation results implied a preponderantly diffusional mechanism in the M $\rightarrow$ γ transformation and a dislocation mechanism in the γ $\rightarrow$ M transformation. The increase of the lattice parameters of maraging steel alloys indicated that the hardening element, which is tungsten, was dissolved after tensile deformation.

1. Introduction

Previous studies [1–3] of dynamic creep applied to steel alloys during the M $\rightleftharpoons$ γ transformation showed that the increase in tensile deformation is referred to the phase change, and to a structural transformation as the precipitation reaction. The majority of these researches dealt with the tensile deformation during precipitation processes [4].

The dynamic creep (creep under thermal cycling) was found to be characterized by an increase in the tensile elongation with time for steel alloys deformed through the phase transition [1, 5–7] as compared to the tensile properties of the equilibrium states.

Until now, dynamic creep deformation in the vicinity of the phase transformation did not yet yield a clear picture of softening [8–11]. The transformation creep strain depended on the strength of the phases that existed during transformation [12, 13] and on the associated dilatometric changes of the transformed phases [14, 15]. On this basis, it is aimed to discuss the dependence of austenite and martensite transformation strain and strain rates in maraging steel alloys on the thermal cycling conditions.

The present work is a study of dynamic creep deformation for three Fe–Ni–Co–W maraging steel alloys during the forward M $\rightarrow$ γ and reverse γ $\rightarrow$ M transformations.

2. Experimental technique

Three maraging steel alloys, Fe–Ni–Co–5 wt % W (referred to as Alloy 1), Fe–Ni–Co–8 wt % W (referred to as Alloy 2), and Fe–Ni–Co–10 wt % W (referred to as Alloy 3), were prepared from a mixture of very pure metallic powders (99.9%) by a sintering method [16]. The materials were rolled in the form of thin sheets of 0.1 mm thickness.

Samples were subjected to different constant applied stresses using a creep testing machine. They were thermally cycled through the M $\rightleftharpoons$ γ transformation with different controlling cycle rates. The heating cycle rates ranged from 8.3×10^{-2} to 16.6×10^{-2} K sec^{-1}, while the cooling rates were $\dot{T}_c = 2\dot{T}_h$). The dynamic tensile deformation was recorded by a tensile gauge with an accuracy of 1 μm.

The structure of the test samples was determined before and after dynamic creep deformation using a D-500 X-ray diffractometer (Siemans, West Germany).

3. Experimental results

The effect of thermal cycling on dynamic creep across the M $\rightleftharpoons$ γ transformation is shown in Figs 1 and 2. Fig. 1 shows the dynamic creep deformation for each alloy during two cyles, the first cycle and the cycle just before rupture. Fig. 2 gives the total tensile strain during the thermal cycle for Alloy 2. It was noticed that the transformation strains and the total strain increase with increasing both the applied stress and the number of cycles. Figs 3a and b represent the austenite and martensite strains ε_A and ε_M, respectively, against the number of cycles under different constant applied stresses and constant heating and cooling cycle rates. Figs 3c and d represent the austenitic and martensitic strain rates $\dot{\varepsilon}_A = \varepsilon_A/t_A$ and $\dot{\varepsilon}_M = \varepsilon_M/t_M$, respectively (where t_A and t_M are the austenitic and martensitic transformation times, respectively) against the number of cycles under different constant applied stresses and constant heating and cooling cycle rates. These curves indicated that ε_A, $\dot{\varepsilon}_A$ and ε_M, $\dot{\varepsilon}_M$ monotonically increase by increasing the applied stress and the number of cycles.

The effect of the applied tensile stress on the transformation strain rates per cycle is illustrated in Fig. 4. It was found that the austenitic transformation strain rate $\dot{\varepsilon}_A$ was a linearly increasing function with the applied stresses, but the martensitic transformation strain rate $\dot{\varepsilon}_M$ increased non-linearly.

The austenitic and martensitic strain rate sensitivity parameters $(m_A = \partial \ln \sigma/\partial \ln \dot{\varepsilon}_A)$, $(m_M = \partial \ln \sigma/$

0022–2461/86 $03.00 + .12

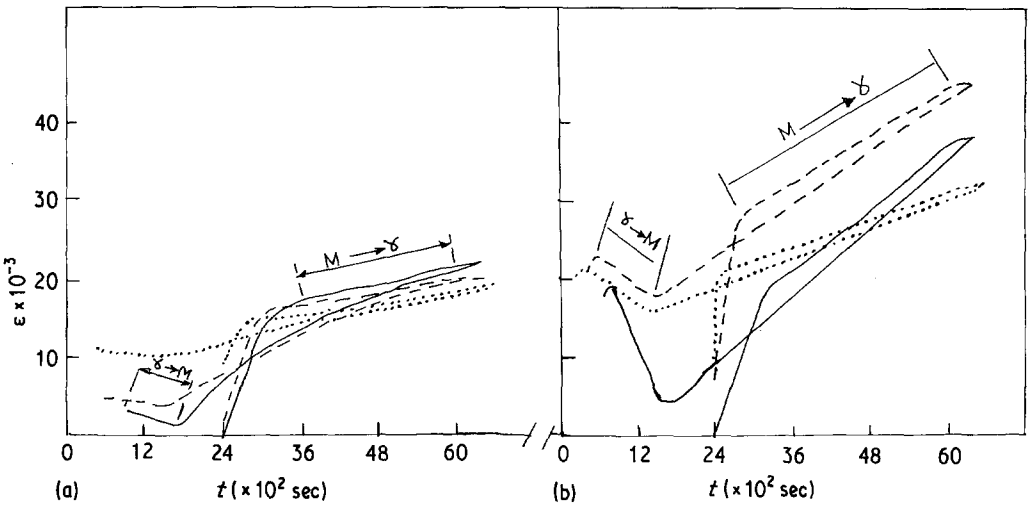

Figure 1 Permanent elongation curves for the three alloys during thermal cycling: (a) first cycle, σ = 2.9 MPa; (b) cycle just before rupture. (———) Alloy 1, (– – –) Alloy 2, (· · ·) Alloy 3; $\dot{T}_h = 8.3 \times 10^{-2}$ K sec^{-1}, $\dot{T}_c = 16.6 \times 10^{-2}$ K sec^{-1}.

$\partial \ln \dot{\varepsilon}_M$) were found from Fig. 4 to be about 1.0 and 0.6, respectively for our three alloys.

Fig. 5 shows the average time of austenitic and martensitic transformations per cycle ($\bar{t}_A$, $\bar{t}_M$) for various constant applied stresses. It was found that both $\bar{t}_A$ and $\bar{t}_M$ decreased by increasing the applied stress and the values of $\bar{t}_A$ (3600 to 2400 sec per cycle) were bigger than those of $\bar{t}_M$ (720 to 360 sec per cycle). $\bar{t}_M$ was not affected by the tungsten content, while $\bar{t}_A$ increased with increasing tungsten content.

The effect of a change in cycling rates on the dynamic tensile deformation is illustrated in Fig. 6 for Alloy 2, which was creep tested under a constant applied stress σ = 28.6 MPa. It was observed that the total strain increased excessively with increasing both the cycling rate $\dot{T}$ and the number of cycles. Fig. 7 represents the relation between the total austenitic and martensitic strains ε_A, ε_M and the number of cycles for different heating and cooling rates, respectively. It was found that both ε_A and ε_M decreased by increasing the cycle

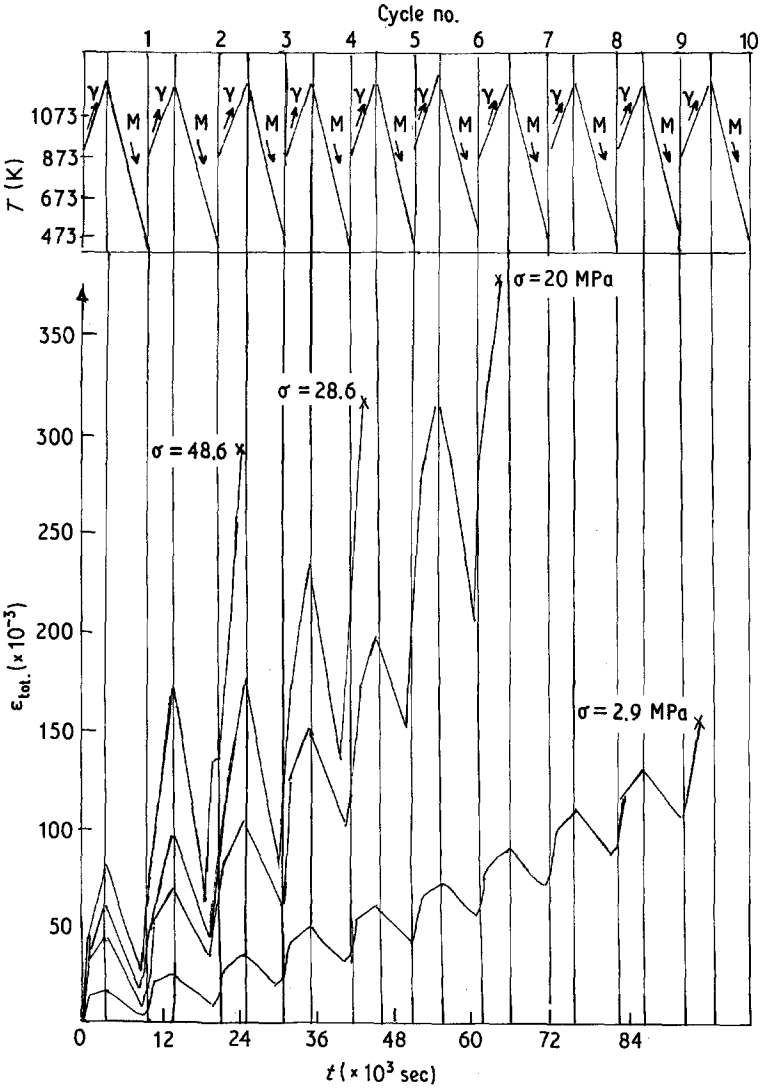

Figure 2 Total strain $\varepsilon_{tot.}$ during thermal cycling under different applied stresses σ (MPa) for Alloy 2, Fe–17.5 Ni–8 Co–8 W (wt %). $\dot{T}_h = 8.3 \times 10^{-2}$ K sec^{-1}, $\dot{T}_c = 16.6 \times 10^{-2}$ K sec^{-1}.

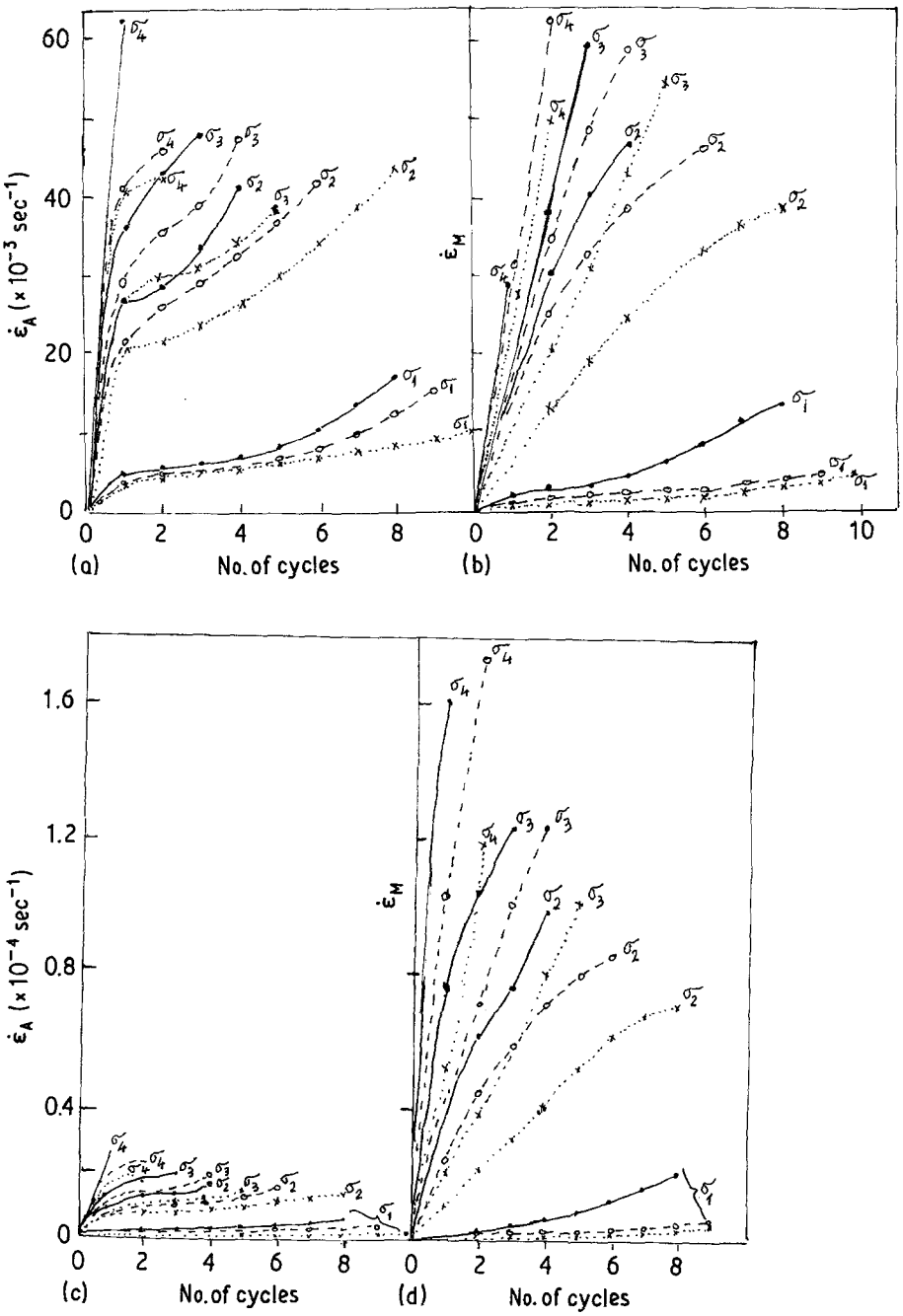

Figure 3 (a, b) Transformation strains ε_A, ε_M and (c, d) strain rates $\dot{\varepsilon}_A$, $\dot{\varepsilon}_M$ for the three alloys. (——) Alloy 1, (– – –) Alloy 2, (· · ·) Alloy 3; $\dot{T}_h = 8.3 \times 10^{-2}$ K sec^{-1}, $\dot{T}_c = 16.6 \times 10^{-2}$ K sec^{-1}; $\sigma_1 = 2.9$ MPa, $\sigma_2 = 20$ MPa, $\sigma_3 = 28.6$ MPa, $\sigma_4 = 48.6$ MPa.

rate, while a non-linear increase of $\dot{\varepsilon}_A$ and $\dot{\varepsilon}_M$ was obtained.

Fig. 8 illustrates the microstructure of the three alloys, i.e. the lattice parameter a, the line width $\Delta(2\theta)$ in degrees and the integral X-ray intensity I of the martensite phase before and after dynamic creep deformation and its variation with the percentage of tungsten. It could be seen that dynamic creep deformation and higher tungsten content in the martensite matrix caused an increase in the lattice parameter a, and the increase of tungsten content resulted in a decrease of both $\Delta(2\theta)$ and I.

4. Discussion

The transformation behaviour of maraging alloys is discussed in the light of the effect of thermal cycle conditions on the tensile deformation (dynamic creep) results.

The superposition of thermal cycling on the test samples even under low stress ($\sigma = 2.9$ MPa) resulted in a continuous increase in dynamic creep strain until fracture (Fig. 1). This would not happen under isothermal conditions, i.e. under constant temperature and constant applied stress. The total dynamic creep strain $\varepsilon_{tot.}$ was affected by the phase transformation $M \rightleftharpoons \gamma$, the weight of tungsten, the applied stresses, the number of cycles, and the heating and cooling cycle rates (Fig. 2). The austenite and martensite transformation strains ε_A, ε_M decreased with increasing percentage of tungsten as a hardening element in the transformed matrix, and increased with increasing both the applied stress and the number of cycles under a moderate constant heating and cooling rate, (Fig. 3). This could be explained in terms of changes in the internal stresses generated at transformation fronts during the transformation reactions. Obviously, increasing the applied stress accelerated the fracture process and the fracture strain rates. A moderate thermal cycle increased the density of mobile point defects in the vicinity of the transformation front for

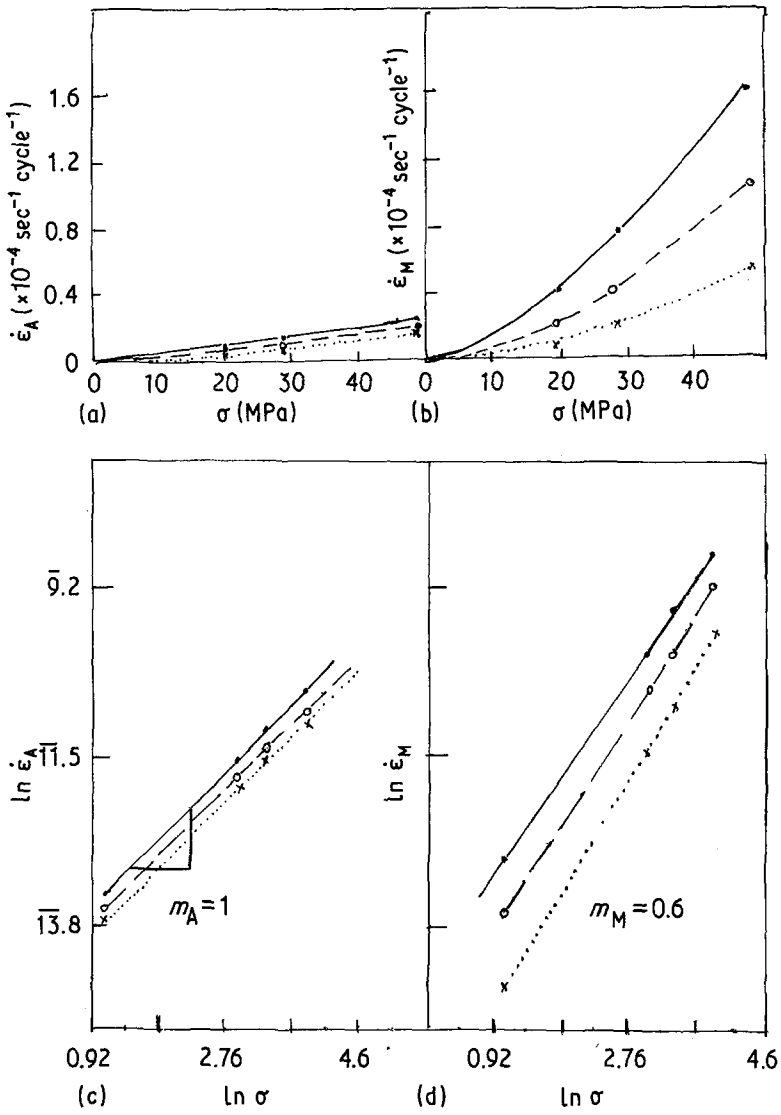

Figure 4 The influence of applied stress during thermal cycling on strain rate of (a, c) austenite and (b, d) martensite transformation for the three alloys. (——) Alloy 1, (– – –) Alloy 2, (· · ·) Alloy 3; $\dot{T}_h = 8.3 \times 10^{-2}$ K sec^{-1}, $\dot{T}_c = 16.6 \times 10^{-2}$ K sec^{-1}.

the forward M → γ transformation, and of line defects in its vicinity for the reversed γ → M transformation, thus contributing to the transformation strain and strain rate. The rate of accumulation of the newly created mobile transformation defects in the vicinity of transformation fronts seemed to exceed that of recovery when the number of cycles was increased (Fig. 3).

The linearity of austenite transformation strain rate $\dot{\varepsilon}_A$ with the applied tensile stress (Fig. 4a) was inferred to the viscous Newtonian flow of the diffusion transformation front of M → γ, where the austenite strain rate sensitivity parameter $m_A = 1.0$ (Fig. 4c). The non-linear behaviour of the martensite transformation strain rate $\dot{\varepsilon}_M$ with applied tensile stress (Fig. 4b) was attributed to dislocation mechanisms in the vicinity of

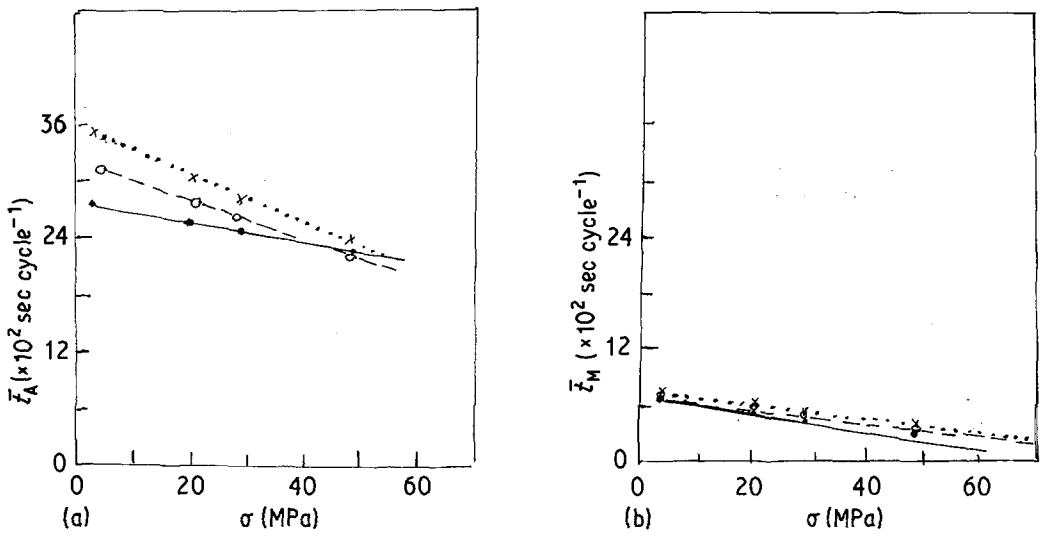

Figure 5 The average transformation time per cycle against applied for the three alloys: (a) austenite transformation time, $\bar{t}_A$, (b) martensite transformation time, $\bar{t}_M$. (——) Alloy 1, (– – –) Alloy 2, (· · ·) Alloy 3; $\dot{T}_h = 8.3 \times 10^{-2}$ K sec^{-1}, $\dot{T}_c = 16.6 \times 10^{-2}$ K sec^{-1}.

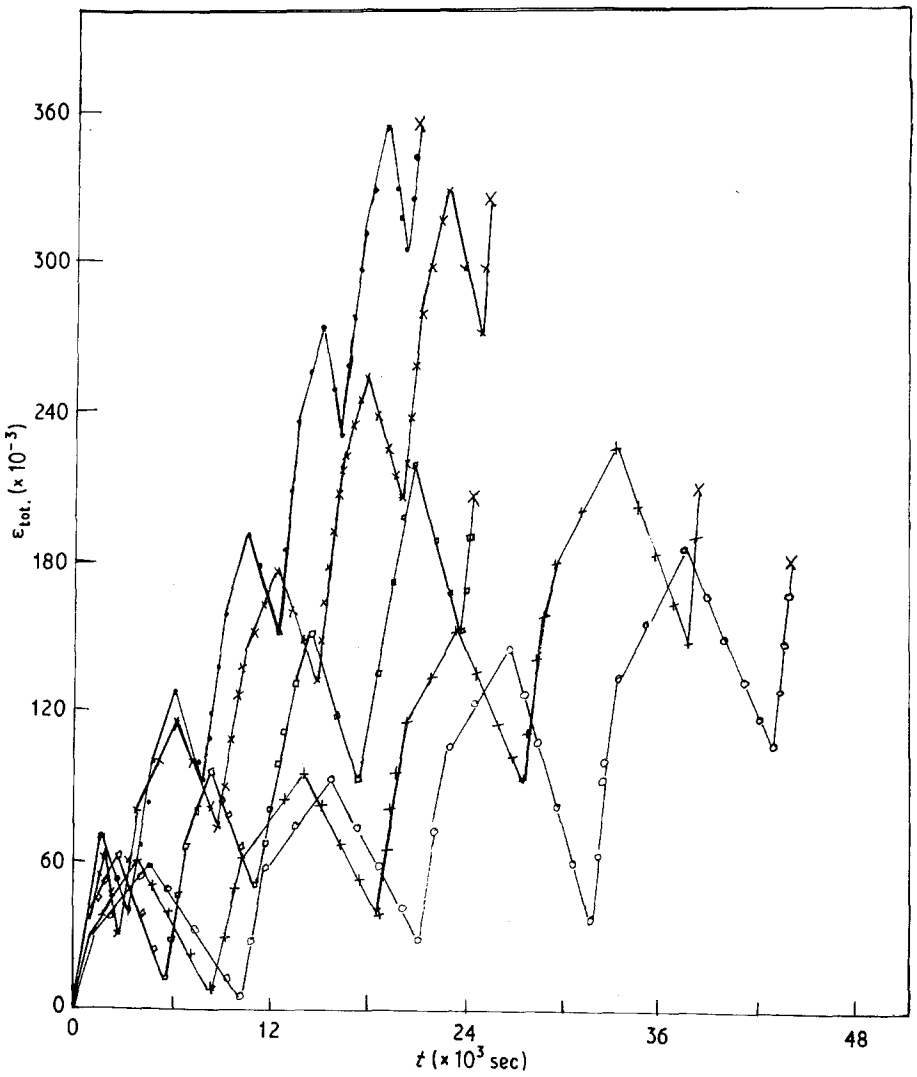

Figure 6 The effect of changing the cycling rates on the dynamic tensile deformation under a constant stress σ = 28.6 MPa, for Alloy 2, Fe–17.5 Ni–8 Co–8 W (wt %). Values of $\dot{T}_h$ ($\times 10^{-2}$ K sec^{-1}) were as follows: (●) 20.8, (×) 16.6, (□) 12.5, (+) 8.3, (○) 6.6. $\dot{T}_c = 2\dot{T}_h$ in all cases.

the dislocation transformation front of $\gamma \rightarrow$ M, where the martensitic strain rate sensitivity parameter m_M is equal to 0.6 (Fig. 4d).

The average time per cycle of austenite and martensite transformation $\bar{t}_A$, $\bar{t}_M$ was found to decrease with increasing the applied stress, which revealed that the applied stress caused enhancement of the transformation fronts.

Increasing the tungsten content resulted in increasing the austenite transformation time $\bar{t}_A$, while it had no effect on the martensite transformation time $\bar{t}_M$ which was shorter than $\bar{t}_A$. This showed that austenite and martensite transformation fronts exhibited diffusion behaviour and dislocation behaviour, respectively.

A considerable increase in the total dynamic strain for Alloy 2 due to the change of the heating and cooling cycle rates $\dot{T}_c = 2\dot{T}_h$ was also observed (Fig. 6). The non-linear behaviour of the austenite and martensite transformation strain rates $\dot{\varepsilon}_A$, $\dot{\varepsilon}_M$ with the rate of change in temperature $\dot{T}$ and the number of cycles (Fig. 7) was attributed to the supersaturation of point defects in the vicinity of transformation fronts that enhances the climb and slipping of dislocations in austenite and martensite transformed matrices, respectively.

The present structural results (Fig. 8) showed that the lattice parameter of lath martensite of b c c structure increases with increasing percentage of tungsten, and after dynamic creep deformation. This was a result of the distortion and partial dissolution of tungsten precipitates A_3W by the dynamic creep deformation, which increases the homogeneity of tungsten in the martensitic matrix.

The decrease in the integral intensity I and the increase in the line width $\Delta(2\theta)$ of the X-ray diffraction pattern for the martensitic matrix, after dynamic creep tests, indicated that the residual internal strains increased appreciably in the martensite after being supersaturated with a high dislocation density due to dynamic creep deformation.

Acknowledgements

The authors would like to thank Professor P. Lacombe, Dr C. Servant and all members of Laboratorie de Metallurgie Physique, Université d'Orsay, Paris-Sud, for their collaboration and some experimental facilities which they provided.

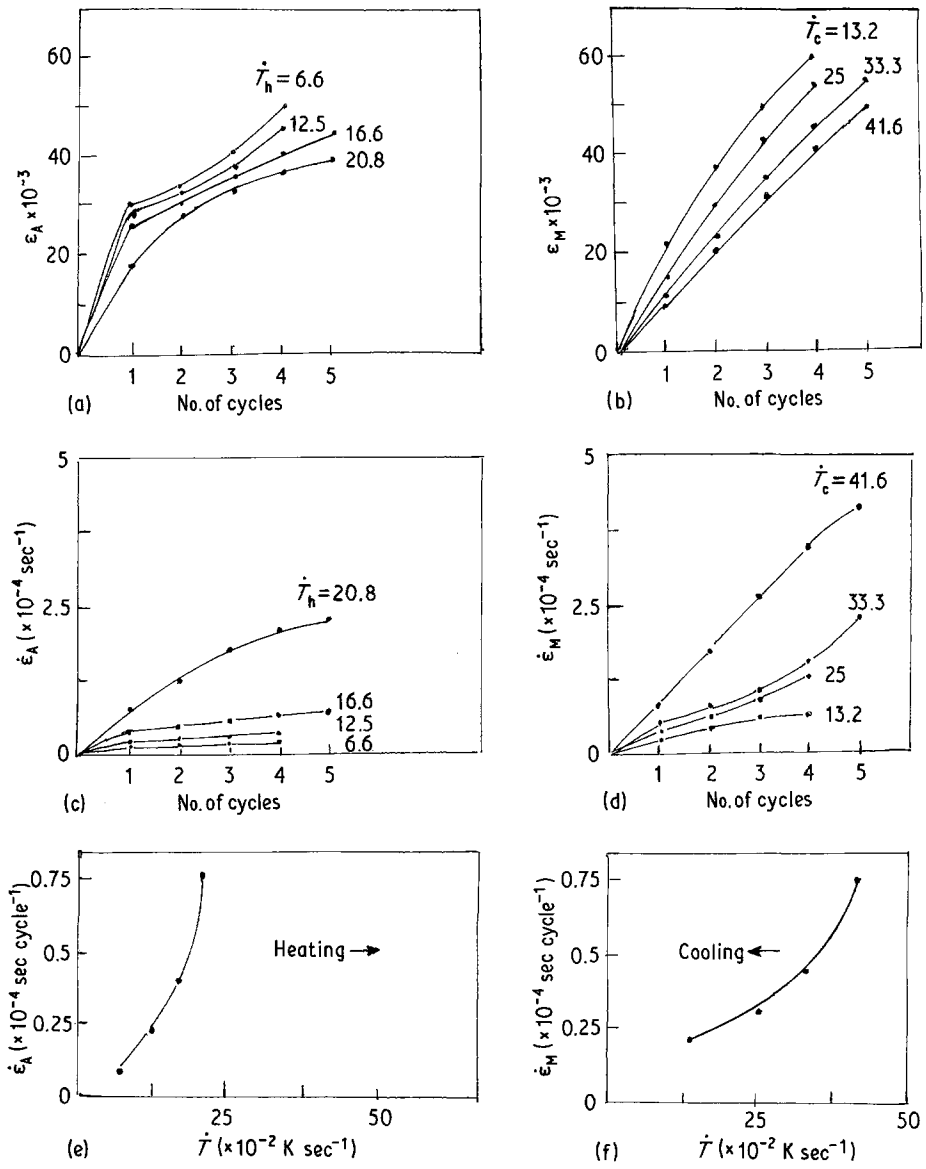

Figure 7 The effect of cycling rate and number of cycles on the strain and strain rate of austenite and martensite transformation for Alloy 2, Fe–17.5 Ni–8 Co–8 W (wt %) at σ = 28.6 MPa.

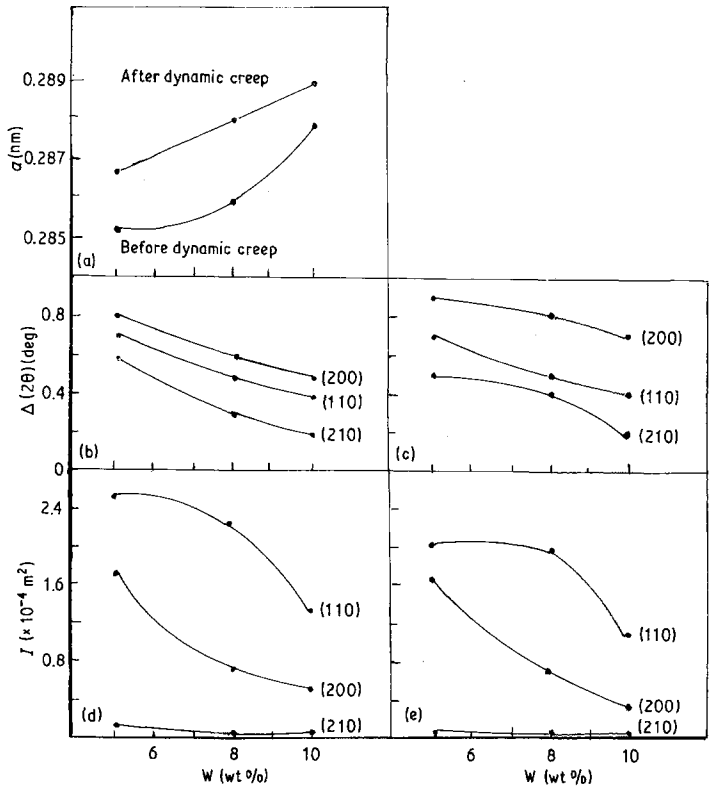

Figure 8 The variation of lattice parameter, *a*, X-ray line width, $\Delta(2\theta)$ and integrated intensity, *I*, with the percentage of tungsten in the martensite phase: (b, d) before dynamic creep, (c, d) after dynamic creep.

References

1. G. J. DAVIS, J. W. EDINGTON, C. P. CUTLER and K. A. PADMANABHAN, *J. Met. Sci.* **5** (1970) 1091.
2. J. R. C. GUIMARAESS and R. J. DE ANGELIS, *Met. Trans.* **4** (1973) 2379.
3. J. R. DONOSO, P. G. WATSON and R. E. REED-HILL, *ibid.* **10A** (1979) 1165.
4. O. V. ABRAMOV, A. I. ILLIN and V. M. KARDONSKII, *Metallov. Termiches. Obra. Metall.* **4** (1981) 31.
5. D. OELSCHLAGEL and V. WEISS, *Trans. ASM* **59** (1966) 143.
6. R. KOT and V. WEISS, *ibid.* **60** (1967) 566.
7. F. W. CLIMARD and O. D. SHERBY, *Acta. Metall.* **2** (1964) 911.
8. M. D. PERKAS and V. M. KARDONSKII, "High Strength Maraging Steel" (in Russian) (Metallurgiya, Moscow, 1970) p. 176.
9. Ya-M. POTAK, "High Strength Steels" (in Russian) (Metallurgiya, Moscow, 1972) p. 55.
10. R. C. GRIFKINS, *J. Mater. Sci.* **13** (1978) 1962.
11. J. R. SPINGARN and N. D. NIX, *Acta Metall.* **26** (1978) 1389.
12. V. K. SHARMA and N. V. BREYER, *Met. Trans.* **5** (1) (1974) 301.
13. P. DOIG and P. E. J. FLEWITT, *Phil. Mag.* **35** (1977) 1063.
14. C. SERVANT, G. MAEDER and P. LACOMBE, *Met. Trans.* **10(A)** (1979) 1607.
15. C. SERVANT and P. LACOMBE, *J. Met. Sci.* **12** (1977) 1807.
16. C. SERVANT, thése de doctorat d'état, Université de Paris-Sud, Orsay (1972).

Received 29 February
and accepted 23 October 1985